

35. DATA REPORT: INORGANIC MAJOR, TRACE, AND RARE EARTH ELEMENT ANALYSES OF THE MUDS AND MUDSTONES FROM SITE 808¹

Kevin T. Pickering,² Nicholas G. Marsh,² and Brian Dickie²

OBJECTIVES

The principal aims of undertaking a shore-based bulk inorganic geochemical analysis of muds and mudstones from Site 808 were as follows:

1. Characterize the geochemical signature of the muds and mudstones at regular intervals downhole to sample and identify any changes in sediment type and provenance.
2. Integrate the inorganic geochemistry with the shipboard and more detailed land-based laboratory studies of the clay minerals.
3. Investigate any possible inorganic geochemical anomalies associated with the décollement.

ANALYTICAL TECHNIQUES

Major- and trace-element analysis of the samples was carried out at the University of Leicester Department of Geology by X-ray fluorescence (XRF) spectrometry using an ARL8420+ XRF spectrometer and a Philips PW1400 XRF spectrometer. Inductively coupled plasma/optical emission (ICP/OE) spectrometry was used to determine a more complete range of rare earth elements (REE). These analyses were carried out on the University of Leicester Department of Geology Philips PV8060 simultaneous ICP/OE spectrometer. Due to the small amounts of material available for many of the samples, the techniques developed and routinely used at Leicester for geochemical analysis of igneous samples from DSDP and ODP Legs had to be modified (see, for example, Marsh et al., 1980, Marsh et al., 1983, Saunders et al., 1991, Tarney and Marsh, 1991). Hence, a more detailed description of the methodology is presented.

SAMPLE PREPARATION

All samples were checked against the original sample lists and then given an abbreviated laboratory number that also introduced a degree of randomization to the sample processing order. All samples were then dried overnight at 105°C after removal from their plastic sampling tubes where necessary. The samples were then crushed to an average particle size of between 1 and 2 mm by crushing between the hardened steel faces of a "fly-press." Previous work with igneous and metamorphic rocks has shown contamination to be minimal by this technique. Due to the small amounts of material available, the routine crushing technique of using an agate swing mill was not viable. Hence the "fly-pressed" samples were crushed for 35–40 min in a Fritsch Pulverisette agate vibratory ball pestle and mortar to reduce the samples to fine powders (average grain size <200 µm mesh). The resultant fine powders were then dried again overnight at 105°C. Prior to use for XRF sample preparation or ICP/OES REE analysis sample digestion, the samples were ignited in platinum cru-

cibles in a vented muffle furnace at 950°C for 90 min. Losses on ignition were determined and are included in the data tables. The data for other elements have been recalculated to include the loss on ignition values.

XRF ANALYSIS

Major elements were determined on fusion disks prepared as follows. 1 g of ignited (volatile-free, fully oxidized) sample was fused with 5 g of Englehard Standard XRF grade Flux, an 80:20 mix of lithium metaborate and lithium tetraborate (equivalent to Johnson Matthey Spectroflux JM100B) for 20 min at 1100°C with intermittent swirling to ensure thorough mixing. The resultant melt was cast and pressed between the polished aluminum faces of a press, similar to the technique described by Harvey et al. (1973). The resultant fusion disks were then annealed at 250°C for a minimum of 3 hr. Analysis was performed on the University of Leicester Department of Geology ARL8420+ XRF spectrometer running a 3-kW rhodium anode X-ray tube at 50 kV 50 mA. Full analytical details are given in Table 1. Note that with the improved resolution of this spectrometer's design, it is possible to analyze for P using the P K α peak and pentaerythritol 002 (PET) as the analyzing crystal with no detectable overlap from the second order Ca K β peak or its escape peak without having to resort to using Ge₁₁₁.

The count data were collected on a dedicated IBM Series 2/70 computer and processed using ARL386 Phase 1 software. Calibrations have previously been produced from data collected on some 65 international reference materials and computing Traille-Lachance-based correction coefficients using the ARL386 software regression package. Values for the concentrations of the reference materials were taken from Govindaraju (1989).

Table 2 lists results for selected reference materials run at the same time as the samples to allow the estimation of precision and accuracy of the results. Our laboratory generally applies a quality control filter on major element analyses, only taking analyses with totals between 99.00% and 100.50% as acceptable. If analyses fall outside this range repeat fusion disks are prepared and analyzed. If the repeat analyses are within the acceptance range they are then used, or if triplicate beads reproduce analysis results within the expected precision range for each component, then the mean analysis for the triplicates is accepted in the event of totals falling below the acceptable range. Unfortunately the lack of sample in most cases precluded our usual quality checking, and in virtually all cases, the first-attempt analysis has had to stand. Certain samples did not have sufficient material to provide 1 g of ignited material for the fusion disk preparation described above. In these cases 0.5 g of ignited powder and 0.5 g of Koch Chemicals 99.999% SiO₂ were used to make fusion disks. The resulting analysis then had the error of the total from 100% split 50:50 between 50.00% of the SiO₂ content and the remainder of the component concentrations. The error-corrected 50% SiO₂ was then subtracted from the total SiO₂ content and the remaining SiO₂ content and other component concentrations were then doubled to generate the "sample" analysis. Blanks with just the Koch Chemicals 99.999% SiO₂ were also made to ensure that no detectable contamination from other elements was being introduced.

¹ Hill, I.A., Taira, A., Firth, J.V., et al., 1993. *Proc. ODP. Sci. Results*, 131: College Station, TX (Ocean Drilling Program).

² Department of Geology, University of Leicester, Leicester LE1 7RH, United Kingdom.

Table 1. Analytical conditions for major-element analysis of fusion disks on the University of Leicester Department of Geology ARL8420+ XRF spectrometer.

Element	Line	Crystal	Peak angle	Count time (s)	Background 1 angle	Count time (s)	Background 2 angle	Count time (s)	Collimator	Detector
Goniometer 1										
P	Ka1,2	PET	89.54	50	91.97	25	86.7	25	Fine	FPC
Si	Ka1,2	PET	109.21	20	112.44	5	105.57	5	Std. Coarse	FPC
Al	Ka1,2	PET	145.12	30	148.85	15	140.44	15	Std. Coarse	FPC
Mg	Ka1,2	AX06	20.2	50	22.25	20	18.98	20	Std. Coarse	FPC
Na	Ka1,2	AX06	24.37	50	26.99	20	22.25	20	Std. Coarse	FPC
Goniometer 2										
Fe	Ka1,2	LiF200	57.52	25	60.42	10	55.25	10	Fine	FPC
Ti	Ka1,2	LiF200	86.14	40	88.8	20	84.25	20	Fine	FPC
Ca	Ka1,2	LiF200	113.09	25	115.1	10	110.1	10	Fine	FPC
K	Ka1,2	LiF200	136.69	50	139.36	20	131.67	20	Fine	FPC
Mn	Ka1,2	LiF220	95.2	50	98	25	92.85	25	Fine	FPC

Trace elements are routinely determined on pressed powder briquettes in our laboratory. Yet again the small amounts of material available precluded this approach. As a result, trace-element determinations were made on the fusion disks. Nb, Zr, Y, Sr, Rb, Ga, Zn, Ni, and Th were analyzed on the Philips PW1400 using a 3-kW Cr anode X-ray tube operated at 80 kV 30 mA. Sc, V, Cr, Co, Cu, Ba, La, Ce, and Nd were analyzed on the ARL8420+ using a 3 kW Rh anode X-ray tube operated at 60 kV 45 mA. The following overlaps were corrected for Sr K β on Zr K α , Rb K β on Y K α , Ti K β on V K α , followed by corrected V K β on Cr K α , Fe K β on Co K α , and the mutual overlap of Ce Lb₁ and Nd La₁ on each other. Although Ba is determined on the La₁ line, use of LiF₂₂₀ on the ARL8420+ gives a line free from interference from both Ti K α and Sc K β at the concentration levels found in most geological samples. Similarly, the Sc K α peak is free from overlap of Ca K β at the concentrations of Ca found in most geological materials except limestones, some high Ca dolostones, and high Ca marbles.

Details of analytical conditions for each element are given in Table 3. Mass absorption correction was performed using mass attenuation coefficients calculated at each analyte wavelength from the major-element analyses and the values tabulated by Thin and Leroux (1979). Calibrations were prepared from the fully corrected count data collected on 51 International Reference materials using the values given by Govindaraju (1989) except that for values of Zr and Nb the values given by Jochum et al. (1990) were used in preference. Table 4 gives details of precision and allows a comparison of accuracy for trace element determinations performed on a selection of reference materials analyzed with the samples. Table 5 gives the XRF analyses for the Site 808 samples.

While most of the samples analyzed fell well within the range of materials and concentration ranges covered by our selection of International Reference materials, this is not the case for Samples 131-808C-83R-2, 57–58 cm, 131-808C-85R-1, 59–61 cm, and 131-808C-86R-2, 110–112 cm. Accordingly, the results quoted for these samples should be treated with a greater degree of caution.

ICP ANALYSIS

Simultaneous analysis of the REE was carried out using the University of Leicester Department of Geology Philips PV8060 ICP optical emission spectrometer. The technique is essentially the same as that described by Walsh et al. (1981); 0.5 g of ignited powder for each of the selected samples was digested in open PTFE beakers by 15 mL HF plus 4 mL HClO₄, followed by an additional 4 mL aliquot of HClO₄ on reaching incipient dryness, to ensure complete removal of excess HF and Si complexes. On drying to incipient dryness again, the samples are taken up in 20 mL of 25% HCl and then diluted to 50 mL with reverse osmosis/deionized H₂O prior to the REE's being separated by ion exchange chromatography in batches of 10, each batch accompanied by two out of three reference materials (JB-1a,

SO-1, and SO-2) and a reagent blank. The columns used for the reference sample and reagent blank were selected at random for each batch. All the samples from each batch including the reagent blanks and the reference materials were analyzed in one group on the ICP spectrometer. The reagent blanks in each case showed no detectable contamination for REE's in all cases. Results for the reference materials are listed in Table 6, and the analyses are given in Table 7.

RESULTS AND CONCLUSIONS

Figure 1 presents the major and trace elements as abundance normalized to Al₂O₃ vs. depth, because all the analyzed samples were muds or mudrocks. The late stage at which the analyses presented in this report became available for integration into the other Leg 131 geochemical and mineralogical data sets, both from the aqueous phase geochemistry and clay mineralogical studies, preclude a rigorous interpretation of the significance of the data. Some preliminary interpretations are made elsewhere in this volume (Underwood et al., a,b, this volume).

In summary, the initial principal conclusions are as follows:

1. Throughout Site 808, from the deepest Shikoku Basin hemipelagites to the youngest trench and slope muds, the bulk geochemical signature remains essentially uniform, apart from the interval at about 1060–1110 m below seafloor (mbsf) (Fig. 2). The inference from this is that the main sediment source for the muds remained constant over the past 14 m.y., i.e., from the Izu Collision Zone and the mainland Japan or Honshu arc.
2. The décollement is not marked by a significant change in the major- or trace-element inorganic geochemistry of the muds.
3. The décollement is associated with an anomaly in the heavy REE relative to the lighter REE (the subject of further current research). The enhanced heavy REE are associated with otherwise typical muds. A potential candidate for supplying the enriched REE abundances associated with the décollement could be the amber-like metalliferous sediments between about 1060 and 1110 mbsf (see below), i.e., their subcreted equivalents. Subcretion of this material, associated with the complete smectite-illite transformation to release low-chloride fluids and the changing Eh-pH/P-T conditions, may have combined to mobilize the rare earth elements from the ambers. As these postulated fluids moved along the overpressured, dynamically sealed, décollement toward the toe of the accretionary prism, the changing physicochemical conditions may well have induced substantially decreased solubilities for the heavy REE in particular, and therefore led to their preferential adsorption within the hemipelagic muds in the décollement.
4. At about 1060–1110 mbsf, there is an interval of brown muds enriched in Ca, Fe, Mg, Mn, and P oxides, plus several trace elements, particularly Y, Sr, Th, Sc, Cu, Ba, and the REE (Figs. 1–3). We interpret

this interval as an umber, probably created by hydrothermal circulation above the Shikoku Basin spreading center at about 12–10 Ma during the last phase of north-south extension in the Shikoku Basin (Chamot-Rooke et al., 1987). These sediments appear similar to ophiolitic umbers (cf. Robertson and Hudson, 1974) with concentrations of carbonate minerals. At ocean ridge spreading centers, ferromanganous oxyhydroxides, occurring as deep-sea nodules or crusts, readily accommodate the REE (Fleet, 1984).

ACKNOWLEDGMENTS

The authors wish to thank Addy Holmes, Rob Kelly, and Vincent Hilton for all their assistance with sample preparation and aid in preparing this data set. The authors also wish to acknowledge the financial support of the Department of Geology at the University of Leicester, which enabled them to perform these analyses.

REFERENCES*

- Chamot-Rooke, N., Renard, V., and Le Pichon, X., 1987. Magnetic anomalies in the Shikoku Basin: a new interpretation. *Earth Planet. Sci. Lett.*, 83:214–228.
- Fleet, A.J., 1984. Aqueous and sedimentary geochemistry of the rare earth elements. In Henderson, P. (Ed.), *Rare Earth Element Geochemistry*: Amsterdam (Elsevier), 343–373.
- Govindaraju, K., 1989. *Spec. Iss. Geostds. Newsl.*, 13.
- Harvey, P.K., Taylor, D.M., Hendry, R.D., and Bancroft, F., 1973. An accurate fusion method for the analysis of rocks and chemically related materials by X-ray Fluorescence Spectrometry. *X-ray Spectrom.*, 2:33–43.
- Jochum, K.P., Seufert, H.M., and Thirlwall, M.F., 1990. High-sensitivity Nb analysis by spark-source mass spectrometry (SSMS) and calibration of XRF Nb and Zr. *Chem. Geol.*, 81:1–16.
- Marsh, N.G., Saunders, A.D., Tarney, J., and Dick, H.J.B., 1980. Geochemistry of basalts from the Shikoku and Daito Basins. In Klein, G.deV., Kobayashi, K., et al., *Init. Repts. DSDP*, 58: Washington (U.S. Govt. Printing Office), 805–842.
- Marsh, N.G., Tarney, J., and Hendry, G.L., 1983. Trace element geochemistry of basalts from Hole 504B, Panama Basin, Deep Sea Drilling Project Legs 69 and 70. In Cann, J.R., Langseth, M.G., Honnorez, J., Von Herzen, R.P., White, S.M., et al., *Init. Repts. DSDP*, 69: Washington (U.S. Govt. Printing Office), 747–763.
- Nakamura, N., 1974. Determination of REE, Ba, Fe, Mg, Na and K in carbonaceous and ordinary chondrites. *Geochim. Cosmochim. Acta*, 44:1917–1930.
- Robertson, A.H.F., and Hudson, J.D., 1974. Pelagic sediments in the Cretaceous and Tertiary history of the Troodos Massif, Cyprus. In Hsü, K.J., and Jenkyns, H.C. (Eds.), *Pelagic Sediments on Land and Sea*. Spec. Publ. Int. Assoc. Sedimentol., 403–436.
- Saunders, A.D., Storey, M., Gibson, I.L., Leat, P., Hergt, J., and Thompson, R.N., 1991. Chemical and isotopic constraints on the origin of basalts from Ninetyeast Ridge, Indian Ocean: results from DSDP Legs 22 and 26 and ODP Leg 121. In Weissel, J., Peirce, J., Taylor, E., Alt, J., et al., *Proc. ODP, Sci. Results*, 121: College Station, TX (Ocean Drilling Program).
- Tarney, J., and Marsh, N.G., 1991. Major and trace element geochemistry of Holes CY-1 and CY-4: implications for petrogenetic models. In Gibson, I.L., Malpas, J., Robinson, P.T., and Xenophontos, C. (Eds.), *Init. Repts. Cyprus Crustal Study Project*. Pap.—Geol. Surv. Can., 90-20:133–176.
- Thinh, T.P., and Leroux, J., 1979. New basic empirical expression for computing tables of X-ray Mass Attenuation Coefficients. *X-ray Spectrom.*, 8:85–91.
- Walsh, J.N., Buckley, F., and Barker, J., 1981. The simultaneous determination of the rare earth elements in rocks using inductively coupled plasma source spectrometry. *Chem. Geol.*, 33:141–153.

* Abbreviations for names of organizations and publication titles in ODP reference lists follow the style given in *Chemical Abstracts Service Source Index* (published by American Chemical Society).

Date of initial receipt: 23 June 1992

Date of acceptance: 3 September 1992

Ms 131SR-144

Table 2. Mean values and 1-sigma standard deviations for the major elements determined on the ARL8420+ from a selection of reference materials analyzed with the Site 808 samples.

Reference	Sample				BOB-1				NIM-G			
	Mean	Std. dev.	%Std. dev.	Number of runs	Mean	Std. dev.	%Std. dev.	Number of runs	Mean	Std. dev.	%Std. dev.	Number of runs
SiO ₂	50.59	0.1	0.2	10	77.75	0.49	0.63	5	66.06	0.27	0.41	5
TiO ₂	1.29	0.05	0.35	10	0.1	0	0.2	5	0.88	0	0.57	5
Al ₂ O ₃	16.4	0.04	0.24	10	11.52	0.07	0.63	5	14.35	0.05	0.32	5
Fe ₂ O ₃	8.55	0.01	0.16	10	2.02	0.02	1.04	5	7.05	0.02	0.23	5
MnO	0.14	0	0.96	10	0.01	0	15.38	5	0.14	0	0.71	5
MgO	7.66	0.03	0.34	10	0.09	0.01	13.33	5	1.61	0.02	0.99	5
CaO	11.13	0.02	0.21	10	0.75	0	0.4	5	5.68	0.03	0.48	5
Na ₂ O	3.12	0.01	0.4	10	2.91	0.01	0.34	5	3.3	0.03	0.88	5
K ₂ O	0.37	0	0.32	10	4.94	0.01	0.24	5	0.75	0	0.4	5
P ₂ O ₅	0.16	0	0.92	10	0.01	0	6	5	0.17	0	1.21	5
LOI 1	0.73			1	0.63			1	0.38			1
LOI 2					0.59			1	0.34			1

Note: Analyses for BOB-1 were repeated on the same fusion disks and therefore reflect instrumental precision. Analyses for NIM-G, JA-1, SO-1, and SO-2 were performed on three separate fusion disks and reflect the precision of the sample preparation procedures and the instrumental precision. The analyses are reported on a fully oxidized, volatile-free basis.

Table 3. Analytical conditions for trace-element determinations on the University of Leicester Department of Geology Philips PW1400 and ARL8420+.

Element	Line	Crystal	Peak angle (s)	Count time angle	Background 1 (s)	Count time angle	Background 2 (s)	Count time	Collimator	Detector
Nb	Ka1.2	LiF220	30.43	100	33.025	50	29.83	50	Fine Scint.	
Zr	Ka1.2	LiF220	32.115	80	33.025	50	29.83	50	Fine Scint.	
Y	Ka1.2	LiF220	33.925	80	33.025	50	29.83	50	Fine Scint.	
Sr	Ka1.2	LiF220	35.88	80	36.58	50	33.025	50	Fine Scint.	
Rb	Ka1.2	LiF220	38.045	80	38.7	50	36.58	50	Fine Scint.	
Th	La1	LiF220	39.3	100	41.015	50	38.7	50	Fine Scint.	
Ga	Ka1.2	LiF200	38.965	40	39.565	20	38.265	20	Fine	FPC + Scint.
Zn	Ka1.2	LiF200	41.805	40	42.605	20	39.565	20	Fine	FPC + Scint.
Ni	Ka1.2	LiF200	48.625	40	49.885	20	47.125	20	Fine	FPC + Scint.
Ce	Lb1	LiF220	111.64	160	114.07	160	110.14	160	Std. Coarse	FPC
Nd	La1	LiF220	112.67	160	114.07	160	110.14	160	Std. Coarse	FPC
La	La1	LiF220	138.78	160	141.78	80	136.78	80	Std. Coarse	FPC
Ba	La1	LiF220	154.17	100			153.17	100	Std. Coarse	FPC
Fe	Ka1.2	LiF200	57.52	25	60.42	10	55.25	10	Fine	FPC
Ti	Ka1.2	LiF200	86.14	40	88.8	15	84.25	15	Fine	FPC
Co	Ka1.2	LiF200	77.83	100	81.03	40	74.03	40	Fine	FPC
Cr	Ka1.2	LiF200	107.02	100	109.81	40	104.61	40	Fine	FPC
V	Ka1.2	LiF200	123.17	100	126.37	40	121.17	40	Fine	FPC
Sc	Ka1.2	LiF200	97.7	100			95.9	100	Fine	FPC
Ca	Ka1.2	LiF200	113.09	25	115.1	15	110.1	15	Fine	FPC
Cu	Ka1.2	LiF200	45.03	60	45.63	30	44.43	30	Fine	FPC

Table 2 (continued).

JA-1				SO-ISO-2			
Mean	Std. dev.	%Std. dev.	Number of runs	Mean	Std. dev.	%Std. dev.	Number of runs
59.09	0.53	0.9	5	61.47	0.39	0.64	5
0.91	0.01	0.66	5	1.61	0.01	0.37	5
18.13	0.1	0.56	5	16.15	0.1	0.62	5
9.04	0.01	0.14	5	8.96	0.03	0.37	5
0.12	0	1.67	5	0.01	0	10	5
4.1	0.03	0.76	5	1.05	0.02	1.81	5
2.62	0.01	0.57	5	3.01	0.01	0.02	5
2.34	0.02	0.9	5	2.36	0.02	0.97	5
3.28	0.02	0.64	5	3.23	0.01	0.28	5
0.16	0	1.25	5	0.79	0.01	0.76	5
3.9			1	11.07			1
4.02			1	11.42			1

Table 4. Mean values and I-sigma standard deviations for the trace elements determined on the PW1400 and the ARL8420+ from a selection of reference materials analyzed with the Site 808 Samples.

Element	Reference Sample				NIM-G				JA-1				SO-1 SO-2			
	Mean	Std. dev.	%Std. dev.	Number of runs	Mean	Std. dev.	%Std. Dev.	Number of runs	Mean	Std. dev.	%Std. dev.	Number of runs	Mean	Std. dev.	%Std. dev.	Number of runs
Nb	51.51	3.45	6.7	8	7.14	2.42	33.88	5	16.6	2.86	17.22	10	30.34	2.63	8.67	8
Zr	271.57	9.46	3.48	8	85.1	2.52	2.96	5	98.18	3.7	3.77	10	953.28	63.62	6.67	8
Y	152.4	5.56	3.65	8	32.2	2.82	8.8	5	26.55	3.86	14.54	10	54.09	4.75	8.79	8
Sr	11.32	1.27	11.25	8	249.68	1.92	0.77	5	330.92	9.85	2.98	10	356.99	19.35	5.42	8
Rb	324.69	8.6	2.65	8	6.3	1.25	19.9	5	142.97	7.12	4.98	10	78.59	8.49	10.81	8
Th	50.47	3.31	6.57	8	3.5	2.73	78.08	5	19.43	3.53	18.16	10	6.2	4.44	71.53	8
Ga	22.96	2.81	12.25	8	19.86	1.21	6.11	5	19.96	1.7	8.51	10	24.25	1.68	6.92	8
Zn	62.3	1.34	2.15	8	108.8	2.03	1.86	5	181.11	21.16	11.69	10	141.25	4.56	3.23	8
Ni	0.19	0.23	120.55	8	0.72	0.9	125.28	5	97.39	9.62	9.88	10	4.49	2.96	65.89	8
Sc	3.27	2.25	68.79	7	26.3	1.99	7.56	4	18.04	2.43	13.48	7	12.34	2.82	22.87	7
V	1.21	1.67	137.69	7	99.45	2.85	2.87	4	133.21	7.57	5.68	7	64.26	6.61	10.28	7
Cr	14.16	4.49	31.7	7	10.2	3.99	39.16	4	173.83	4.65	2.67	7	13.8	2.37	17.14	7
Co		not detectable		7	17.28	1.54	8.89	4	34.16	1.9	5.56	7	18	1.95	10.81	7
Cu	5.99	1.25	20.86	7	40.45	2.55	6.3	4	62.39	2.94	4.72	7	8.2	2.64	32.22	7
Ba	107.04	3.34	3.12	7	303.42	4.57	1.51	4	949.51	12.04	1.27	7	1153.07	30.47	2.64	7
La	104.84	1.34	1.28	7	4.17	2.29	54.84	4	53.53	2.11	3.94	7	44.71	2.72	6.09	7
Ce	192.79	7.25	3.76	7	11.93	7.24	60.7	4	100.13	5.5	5.5	7	114.71	7.04	6.14	7
Nd	68.91	3.35	4.86	7	9.53	1.64	17.24	4	42.61	4.16	9.77	7	55.37	3.99	7.21	7

Note: Analyses were repeated on the same fusion disks as the major-element determinations and therefore reflect sample preparation and instrumental precision. Note the relatively high standard deviation on the Zr determinations for SO-2. This may reflect a degree of sample inhomogeneity with respect to Zr distribution, perhaps a result of accessory phase control of the Zr content. This problem is not so apparent with the large samples analyzed by conventional powder pellet techniques. The analyses are reported on a fully oxidized, volatile-free basis.

Table 5 (continued).

Sample	Hole, core, section, interval (cm)	Depth (mbsf)	SiO ₂	TiO ₂	Al ₂ O ₃	Fe ₂ O ₃	MnO	MgO	CaO	Na ₂ O	K ₂ O	P ₂ O ₅	LOI	Total
150	808C-85R-1, 59-61	1098.90	20.75	0.241	5.767	5.76	11.939	1.46	22.4	1.27	1.15	15.818	13.87	100.500
139	808C-85R-2, 68-70	1099.59	62.74	0.715	16.26	6.61	0.083	2.44	0.334	1.40	3.47	0.073	4.59	99.090
211	808C-86R-2, 110-112	1110.61	25.32	0.257	6.908	4.59	10.500	1.80	37.6	0.954	1.04	6.212	4.73	100.150
51	808C-87R-1, 78-79	1117.98	62.70	0.694	18.05	6.11	0.076	2.53	0.456	1.36	3.46	0.067	5.04	100.960
190	808C-88R-2, 21-24	1128.62	42.05	0.437	11.20	4.82	2.196	1.84	15.6	1.08	2.22	0.781	15.57	98.070
197	808C-89R-1, 58-60	1137.16	41.03	0.320	12.81	5.72	2.375	2.05	14.9	1.42	1.50	0.141	15.18	96.090
155	808C-89R-1, 126-128	1137.84	56.89	0.636	14.90	5.77	0.249	2.22	5.00	1.28	3.01	0.069	7.71	98.060
154	808C-90R-1, 98-100	1147.29	60.40	0.707	16.11	6.40	0.193	2.46	2.41	1.36	3.16	0.072	5.75	99.330
141	808C-92R-1, 110-113	1166.73	60.84	0.699	15.82	6.28	0.190	2.36	2.10	1.35	3.19	0.072	5.45	98.680
105	808C-92R-CC, 8-10	1167.72	41.58	0.432	10.78	4.70	2.145	1.76	16.6	0.984	2.17	0.369	16.58	98.360
182	808C-93R-1, 76-78	1176.07	62.07	0.704	16.05	6.63	0.191	2.41	0.952	1.33	3.21	0.082	4.76	98.720
50	808C-94R-1, 92-94	1185.83	62.94	0.712	16.38	6.00	0.122	2.27	0.655	1.24	3.43	0.073	5.09	99.360
187	808C-94R-1, 117-119	1186.11	62.01	0.722	16.32	6.60	0.154	2.33	0.865	1.27	3.43	0.068	4.89	99.010
175	808C-95R-1, 22-24	1194.80	61.54	0.732	16.53	6.26	0.122	2.27	1.04	1.26	3.45	0.068	4.87	98.450
79	808C-95R-1, 131-133	1195.89	37.62	0.424	10.70	4.40	1.506	1.52	19.6	0.853	2.25	2.754	16.53	98.370
178	808C-96R-1, 40-42	1204.99	61.74	0.701	16.32	6.71	0.138	2.25	0.715	1.13	3.56	0.081	4.60	98.310
52	808C-97R-1, 45-46	1214.45	60.27	0.687	17.45	6.51	0.292	2.41	1.85	1.27	3.63	0.075	5.97	100.730
129	808C-98R-1-A, 91-92	1224.61	61.34	0.736	16.45	6.85	0.232	2.34	1.78	1.20	3.82	0.742	4.49	100.290
133	808C-98R-1-B, 91-92 siderite?	1224.61	62.55	0.738	16.48	8.12	0.176	2.32	0.470	1.12	4.08	0.084	4.14	100.600
164	808C-99R-1, 86-88	1234.27	61.76	0.698	16.02	7.32	2.210	2.57	0.517	1.23	3.63	0.079	4.35	100.650
198	808C-100R-1, 39-41	1243.40	65.51	0.696	14.37	5.77	0.151	2.24	1.14	1.65	3.26	0.086	3.31	98.690
44	808C-101R-1, 85-87	1253.06	75.65	0.222	11.93	1.59	0.058	0.608	0.646	2.93	2.21	0.154	3.58	100.960
200	808C-101R-3, 55-57	1255.74	73.92	0.230	11.72	1.74	0.063	0.634	0.643	2.89	1.21	0.144	3.96	99.460
9	808C-101R-4, 62-64	1257.31	72.93	0.405	10.86	4.85	0.135	1.41	1.10	1.40	3.09	0.058	3.67	100.260
135	808C-102R-2, 80-82	1263.81	66.84	0.345	7.495	4.68	0.370	1.42	6.31	0.842	3.11	0.118	6.79	98.560
209	808C-102R-3, 133-134	1265.83	65.29	0.160	15.88	1.93	0.138	1.68	2.61	1.46	1.82	0.050	5.85	98.430
173	808C-103R-1, 121-123	1272.14	65.46	0.563	13.12	7.31	0.163	1.95	0.456	1.05	5.66	0.103	2.94	99.030
111	808C-103R-3, 16-18	1274.07	61.88	0.712	15.01	5.89	0.080	2.45	2.44	2.21	2.74	0.122	5.03	99.090
1	808C-103R-3, 40-42	1274.31	70.47	0.406	14.46	1.12	0.047	0.897	2.62	0.924	0.897	0.047	5.64	100.280
109	808C-104R-1, 74-75	1281.15	54.88	0.468	11.68	5.37	0.323	2.15	9.62	1.01	4.25	0.087	10.07	100.210
15	808C-106R-2, 103-108	1301.54	49.08	0.473	12.17	7.01	0.062	2.99	10.7	0.650	6.04	0.098	10.76	100.250
39	808C-106R-2, 103-108	1301.54	49.13	0.472	11.83	7.04	0.062	2.97	10.9	0.705	6.07	0.098	10.97	100.320

Table 5 (continued).

Sample	Hole, core, section, interval (cm)	Nb	Zr	Y	Sr	Rb	Ga	Zn	Ni	Th	Sc	V	Cr	Co	Cu	Ba	La	Ce	Nd
150	808C-85R-1, 59-61	7.8	74.2	482.6	804.0	78.4	4.7	60.8	37.6	19.0	20.0	50.9	22.9	2.5	66.7	8278.6	177.0	235.6	34.7
139	808C-85R-2, 68-70	17.8	164.9	24.2	97.8	166.3	21.7	103.9	63.9	16.0	11.1	132.3	76.7	22.9	60.2	629.0	21.3	64.3	18.8
211	808C-86R-2, 110-112	3.9	99.1	219.0	460.9	55.5	13.0	57.9	34.8	21.4	28.2	57.5	32.4	4.6	60.6	578.4	76.5	154.5	43.7
51	808C-87R-1, 78-79	17.0	149.5	31.1	97.7	142.9	25.7	107.5	49.6	6.9	10.8	124.6	69.5	21.9	72.0	489.4	31.6	61.4	25.4
190	808C-88R-2, 21-24	13.5	103.3	58.2	223.9	103.5	14.6	73.0	42.8	12.2	17.7	96.2	45.8	9.3	74.0	563.6	30.5	72.9	19.9
197	808C-89R-1, 58-60	-1.0	-1.0	-1.0	-1.0	-1.0	-1.0	-1.0	-1.0	-1.0	-1.0	-1.0	-1.0	-1.0	-1.0	-1.0	-1.0	-1.0	-1.0
155	808C-89R-1, 126-128	12.6	139.6	21.7	233.8	147.6	19.1	93.3	31.5	14.0	13.9	110.4	64.3	12.6	66.2	456.4	19.1	55.0	18.9
154	808C-90R-1, 98-100	14.7	149.4	21.8	150.3	149.0	18.7	99.1	23.3	17.1	14.8	112.6	68.5	16.3	60.7	540.0	24.7	64.9	20.3
141	808C-92R-1, 110-113	9.4	141.6	31.4	146.5	152.9	19.8	103.9	50.1	15.1	11.9	111.9	71.5	19.0	66.3	553.6	25.9	70.3	16.4
105	808C-92R-CC, 8-10	8.8	115.1	32.6	186.3	115.7	15.7	71.1	32.3	18.8	19.6	81.0	50.1	9.5	59.3	747.7	23.6	46.4	12.4
182	808C-93R-1, 76-78	12.9	168.4	28.7	103.6	153.5	21.0	103.1	31.3	22.7	15.5	123.7	70.0	15.6	90.0	495.7	27.6	69.6	27.2
50	808C-94R-1, 92-94	18.1	161.3	25.2	97.2	151.5	26.1	104.6	36.8	9.7	12.7	120.6	80.6	17.5	120.1	447.7	25.7	69.2	19.2
187	808C-94R-1, 117-119	17.0	165.1	27.9	106.1	167.1	23.2	105.2	35.3	12.6	11.9	120.9	79.3	16.8	59.0	481.1	24.2	75.5	16.9
175	808C-95R-1, 22-24	16.3	152.8	26.2	104.8	148.5	20.4	102.5	34.7	6.6	14.6	137.6	68.4	14.3	66.3	427.5	28.2	79.3	20.4
79	808C-95R-1, 131-133	10.0	109.4	59.7	252.2	116.7	15.1	81.4	32.9	25.5	20.4	71.3	44.1	10.7	37.7	645.9	48.2	58.9	20.2
178	808C-96R-1, 40-42	15.0	152.3	31.1	92.7	162.6	23.9	105.2	48.4	12.5	13.7	125.1	75.7	21.4	54.3	440.4	30.7	73.5	17.3
52	808C-97R-1, 45-46	14.6	157.5	34.0	117.8	159.7	22.3	111.9	51.2	8.9	15.0	132.4	76.8	18.8	83.0	694.3	35.2	71.2	29.2
129	808C-98R-1-A, 91-92	12.7	183.3	85.4	127.2	210.8	21.9	103.1	35.5	9.2	19.6	134.4	77.7	21.0	113.0	882.1	46.5	141.7	63.3
133	808C-98R-1-B, 91-92 siderite?	14.2	181.0	34.2	98.3	230.8	21.9	98.3	27.3	9.5	15.1	124.2	64.5	18.6	58.8	604.5	31.7	66.5	18.5
164	808C-99R-1, 86-88	16.8	163.8	27.7	87.1	191.3	20.4	110.8	38.1	25.8	10.2	125.5	73.5	21.6	63.0	512.0	23.3	70.8	17.8
198	808C-100R-1, 39-41	11.9	152.1	31.9	104.2	158.0	18.7	79.3	43.7	10.9	13.2	95.2	70.9	17.0	41.2	561.7	22.1	61.0	20.7
44	808C-101R-1, 85-87	8.1	84.0	39.8	58.3	36.6	14.5	45.1	1.7	4.3	3.8	12.7	23.7	0.0	4.9	200.1	17.2	39.9	21.6
200	808C-101R-3, 55-57	11.8	122.7	39.5	72.3	11.2	15.4	34.8	0.0	7.2	4.5	16.1	5.6	0.0	4.2	270.2	12.8	39.4	9.5
9	808C-101R-4, 62-64	5.5	87.5	16.1	89.4	162.5	17.5	84.0	13.1	1.4	7.5	77.7	32.5	8.3	44.4	196.1	15.1	35.5	17.8
135	808C-102R-2, 80-82	5.7	78.6	29.2	218.2	172.4	13.7	62.1	20.2	0.0	10.8	69.7	27.1	8.4	39.3	200.5	20.5	41.3	12.0
209	808C-102R-3, 133-134	27.3	216.8	24.6	806.3	28.8	23.8	46.2	0.0	33.5	5.5	11.9	7.1	0.0	8.9	757.6	29.8	74.3	20.4
173	808C-103R-1, 121-123	11.9	124.0	32.7	49.9	230.0	18.9	91.0	28.5	19.9	10.6	113.0	55.7	14.4	75.6	723.4	22.2	55.9	17.9
111	808C-103R-3, 16-18	17.0	198.7	50.4	73.5	162.9	18.3	95.2	26.2	11.3	16.9	81.9	38.1	10.1	91.8	659.9	23.9	71.1	19.5
1	808C-103R-3, 40-42	8.9	295.4	52.7	785.3	4.0	19.9	26.6	0.0	10.0	11.1	27.0	5.4	0.0	3.4	841.1	25.1	64.7	29.9
109	808C-104R-1, 74-75	11.1	133.6	34.4	320.0	181.9	19.2	86.4	31.4	4.2	13.8	95.2	49.4	15.0	62.4	593.1	17.3	45.2	11.9
15	808C-106R-2, 103-108	15.9	111.0	23.4	260.3	142.5	19.2	88.2	40.8	19.9	16.8	92.6	40.3	18.1	33.7	223.3	24.4	36.8	21.0
39	808C-106R-2, 103-108	10.4	100.1	25.7	262.1	133.5	12.8	92.2	43.2	24.8	13.5	77.0	45.0	20.8	32.3	218.9	24.0	41.2	23.8

Table 6. Mean values and 1-sigma standard deviations for the REE's determined on the PV8060 from the reference materials analyzed with the Site 808 samples.

Element	Reference Sample				JB-1a				SO-1 SO-2			
	Mean	Std. dev.	%Std. dev.	Number of runs	Mean	Std. dev.	%Std. dev.	Number of runs	Mean	Std. dev.	%Std. dev.	Number of runs
La	36.39	3.21	8.83	6	57.98	2.79	4.81	3	50.08	1.05	2.1	2
Ce	62.82	5.01	2.97	6	114.21	5.93	5.19	3	123.48	2.43	1.97	2
Pr	7.47	0.44	5.89	6	13.92	0.65	4.69	3	15.13	0.47	3.11	2
Nd	26.42	2.4	9.06	6	52.73	3.33	6.32	3	63.3	0.68	1.08	2
Sm	4.84	0.32	6.59	6	8.35	0.36	4.33	3	12.74	0.25	1.93	2
Eu	1.55	0.12	7.4	6	1.78	0.1	5.39	3	3.82	0.07	1.79	2
Gd	5	0.5	9.99	6	7.02	0.37	5.26	3	12.11	0.37	3.03	2
Dy	4.33	0.32	7.48	6	5.06	0.23	4.56	3	9.54	0.12	1.26	2
Er	2.47	0.19	7.6	6	2.64	0.09	3.45	3	4.51	0.14	3	2
Yb	1.98	0.16	8.32	6	2.14	0.11	5.24	3	3.46	0.08	2.18	2
Lu	0.3	0.02	5.94	6	0.31	0.02	5.76	3	0.48	0.01	2.68	2

Note: Analyses were for repeated sample preparations and therefore reflect both sample preparation and instrumental precision combined. The analyses are reported on a fully oxidized, volatile-free basis.

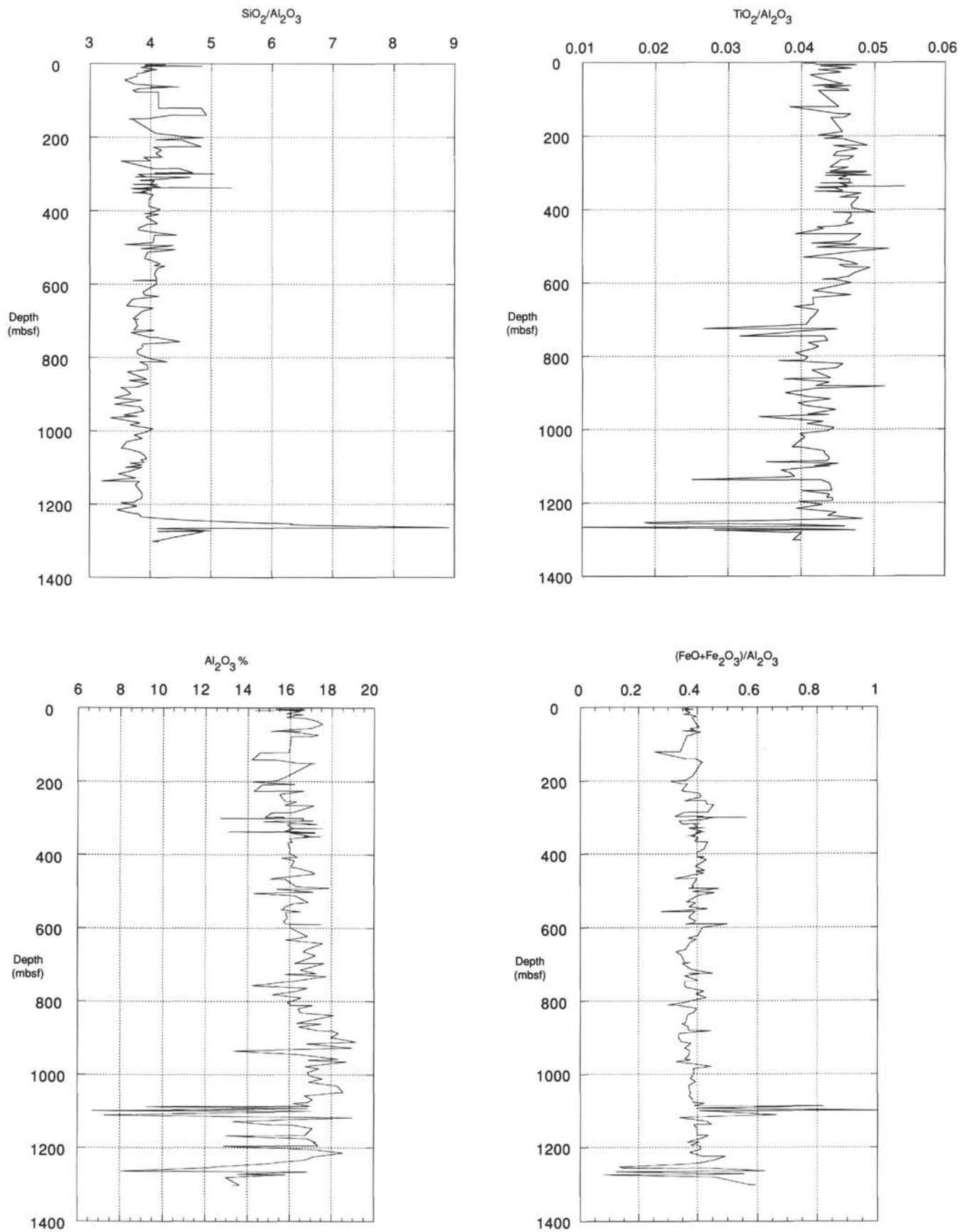


Figure 1. Element and element oxide abundances vs. depth (mbsf) for Site 808. Graphs show element and element oxide abundances normalized to Al₂O₃ vs. depth.

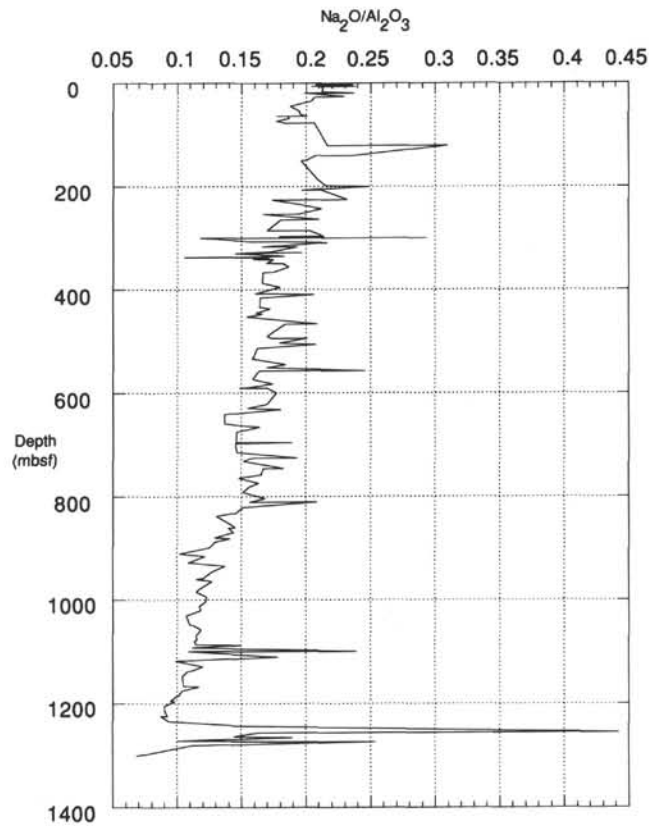
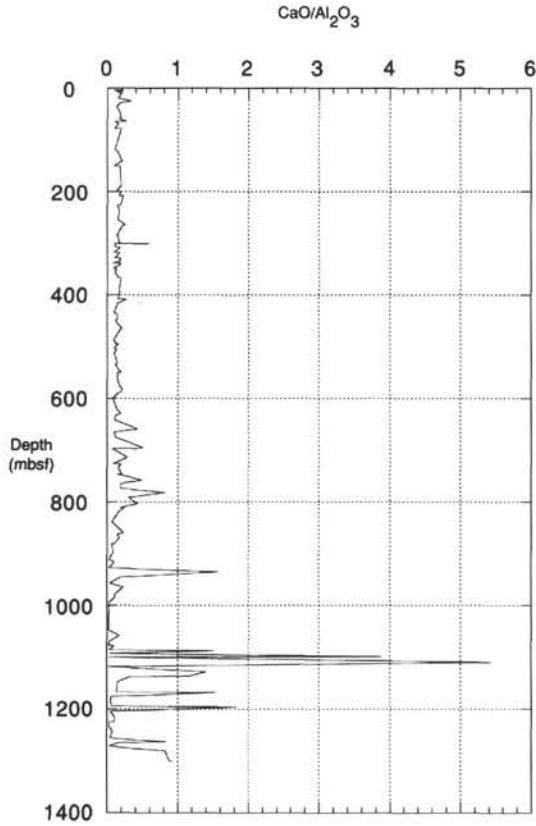
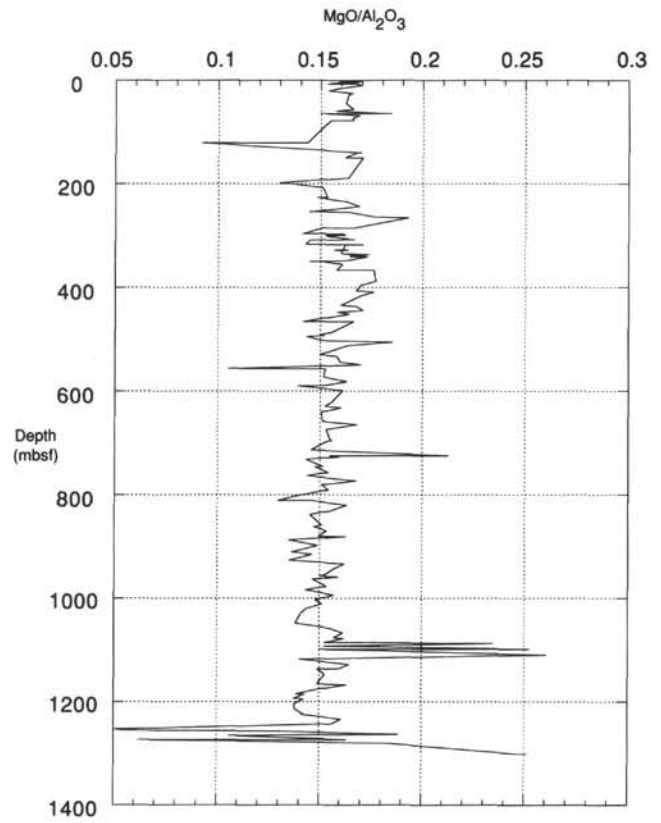
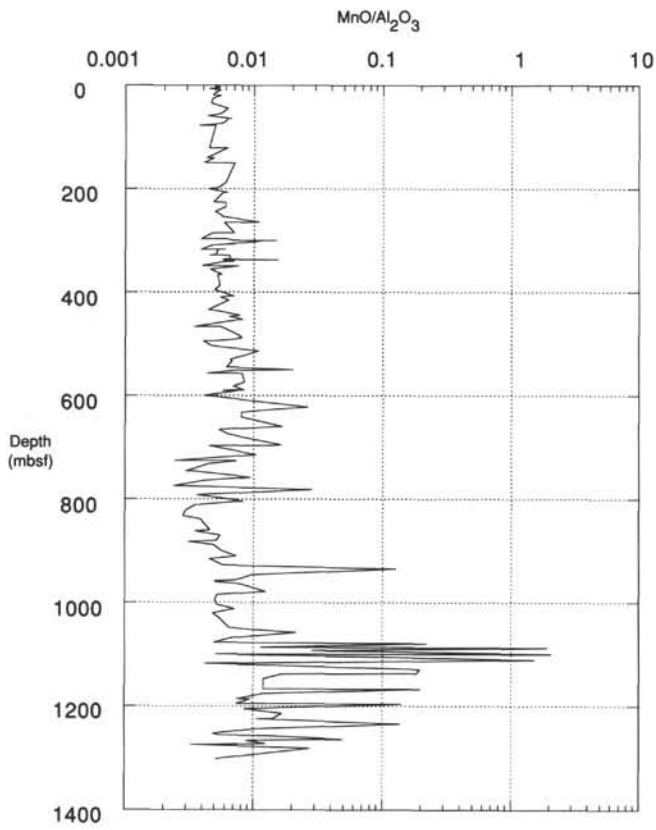


Figure 1 (continued).

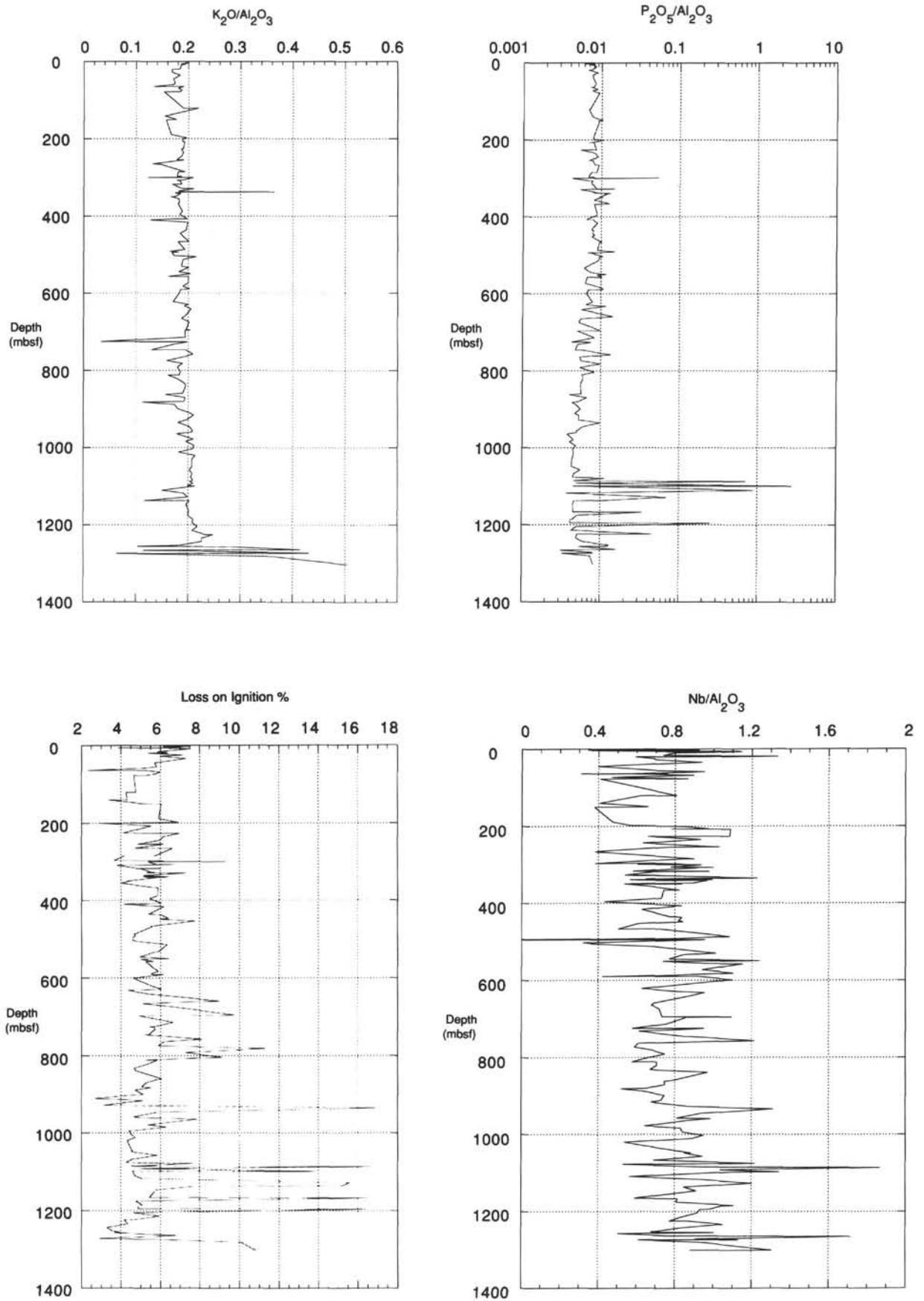


Figure 1 (continued).

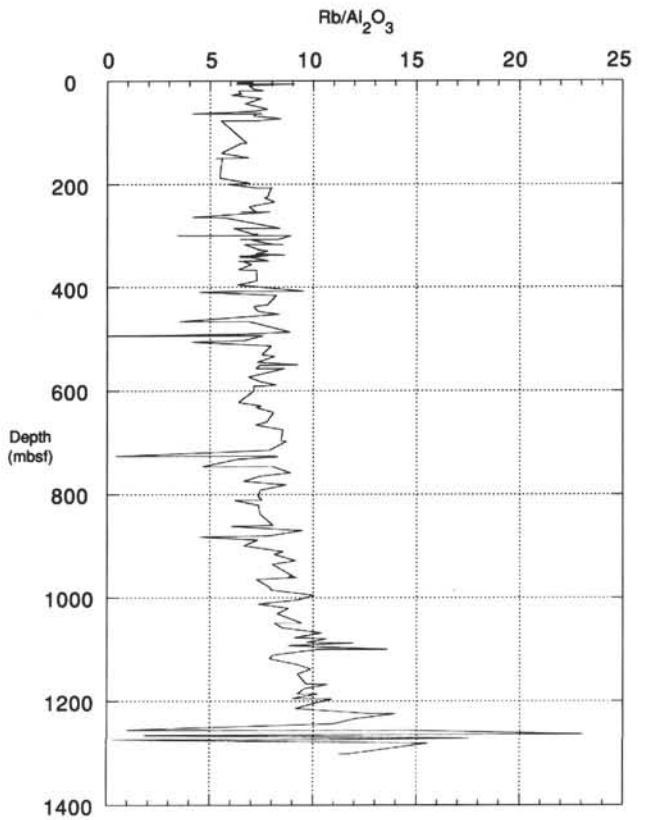
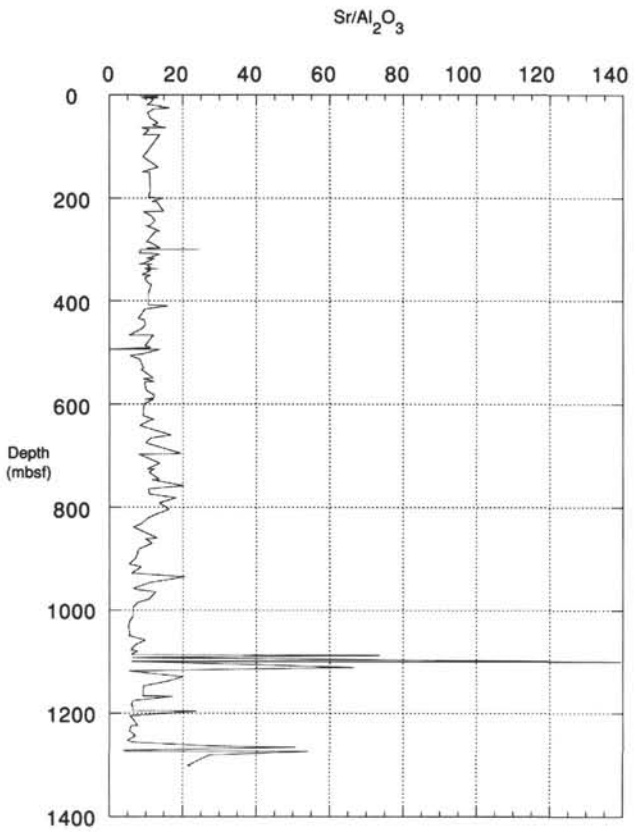
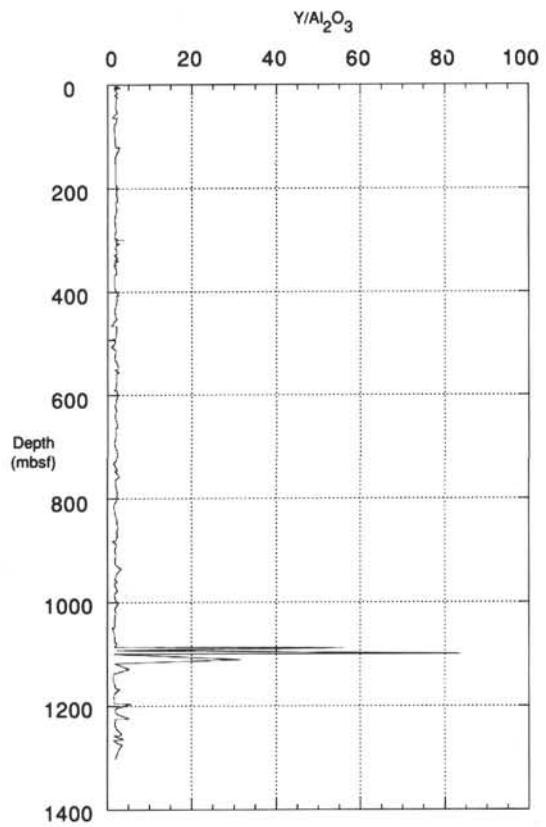
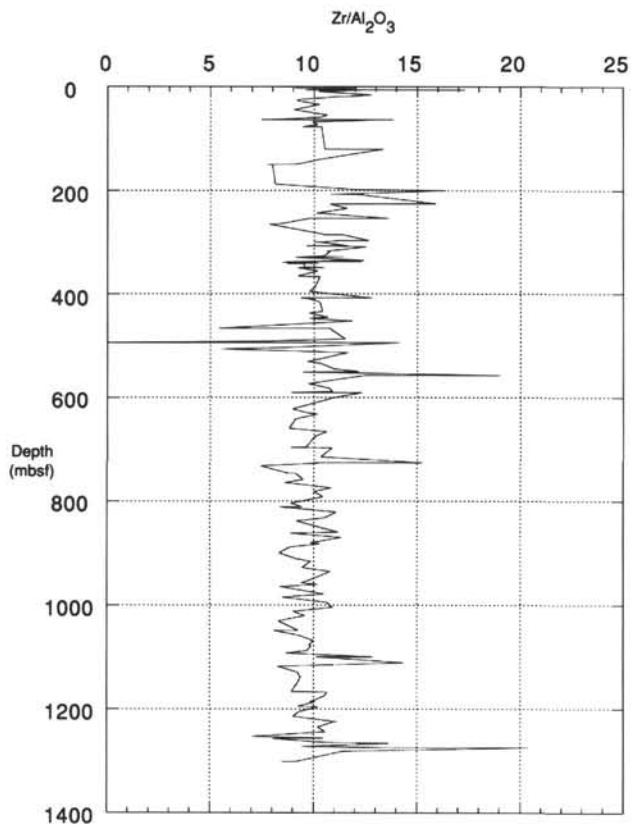


Figure 1 (continued).

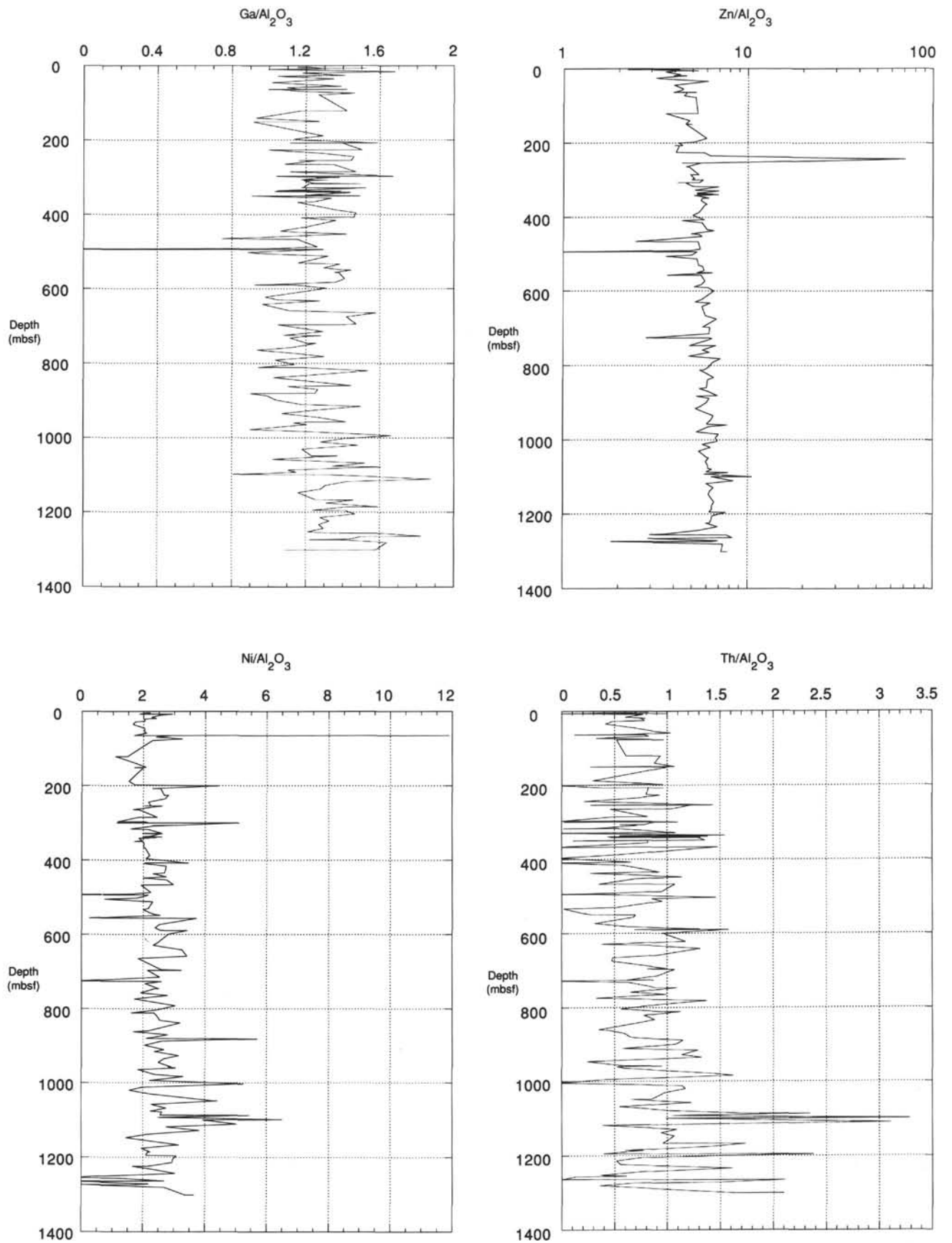


Figure 1 (continued).

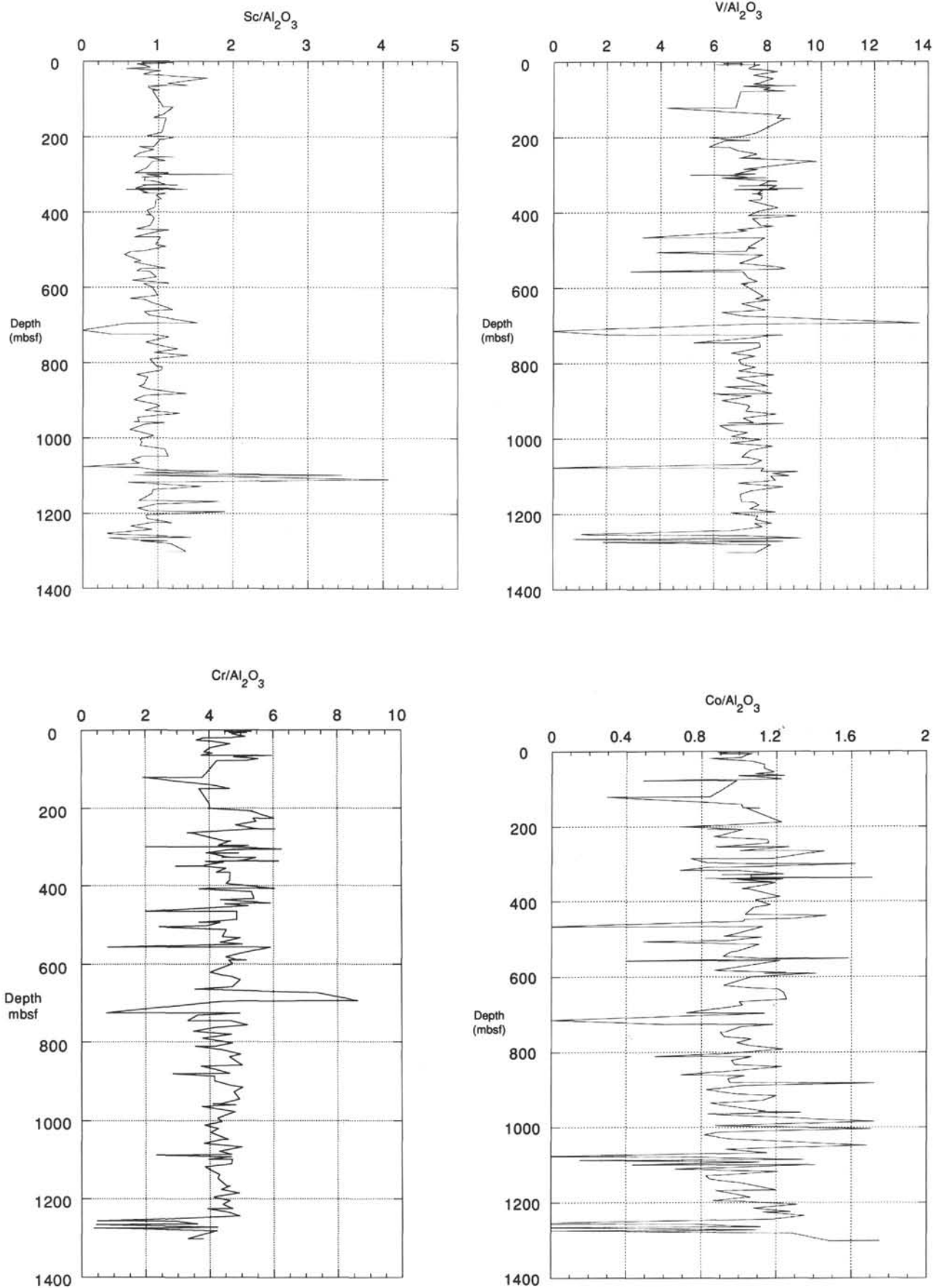
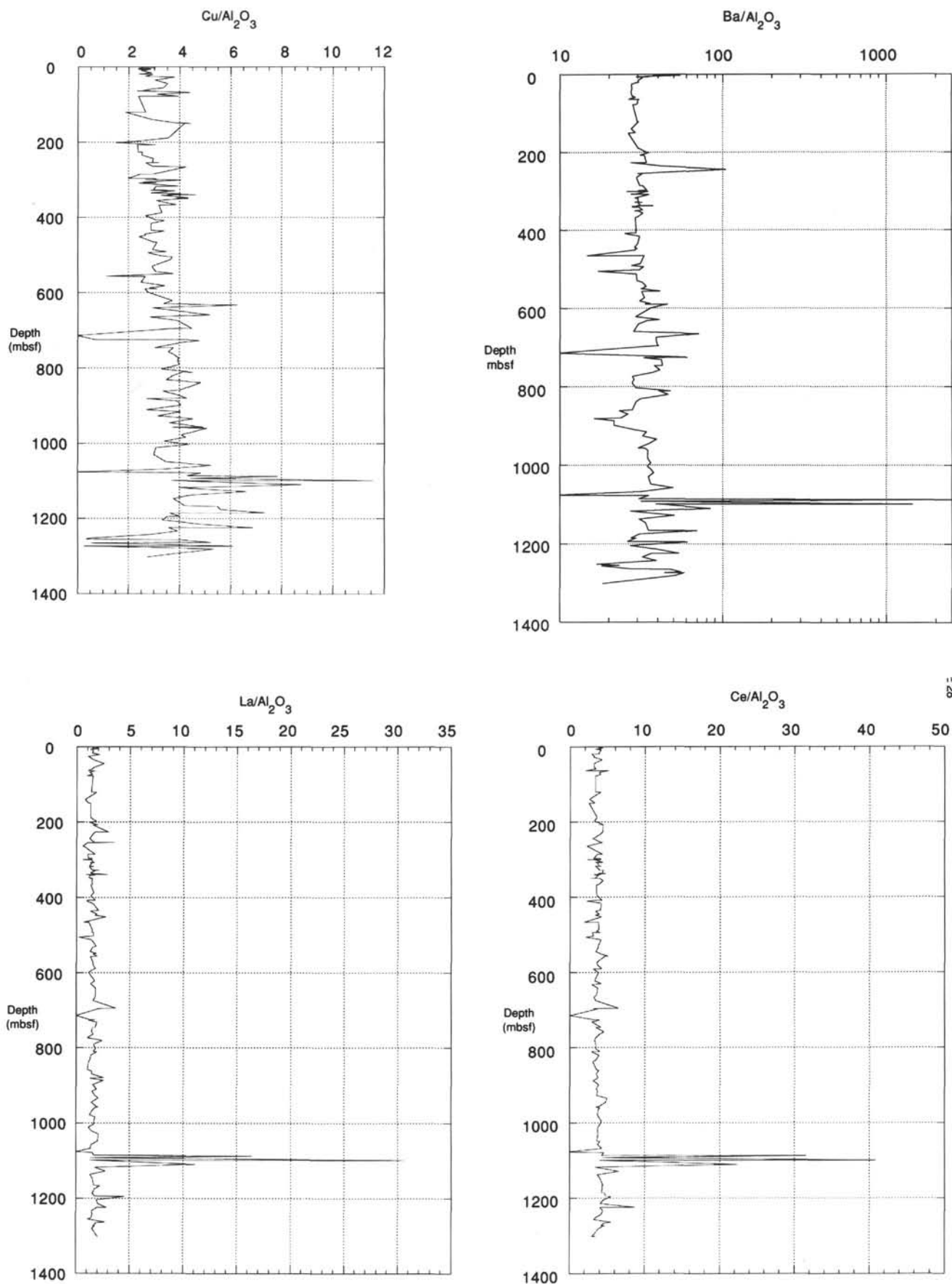


Figure 1 (continued).



28

Figure 1 (continued).

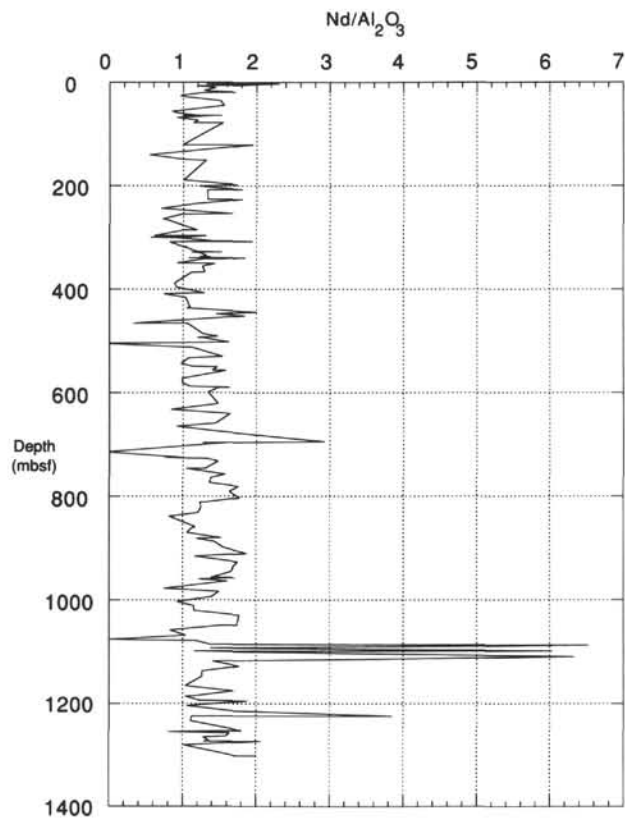


Figure 1 (continued).

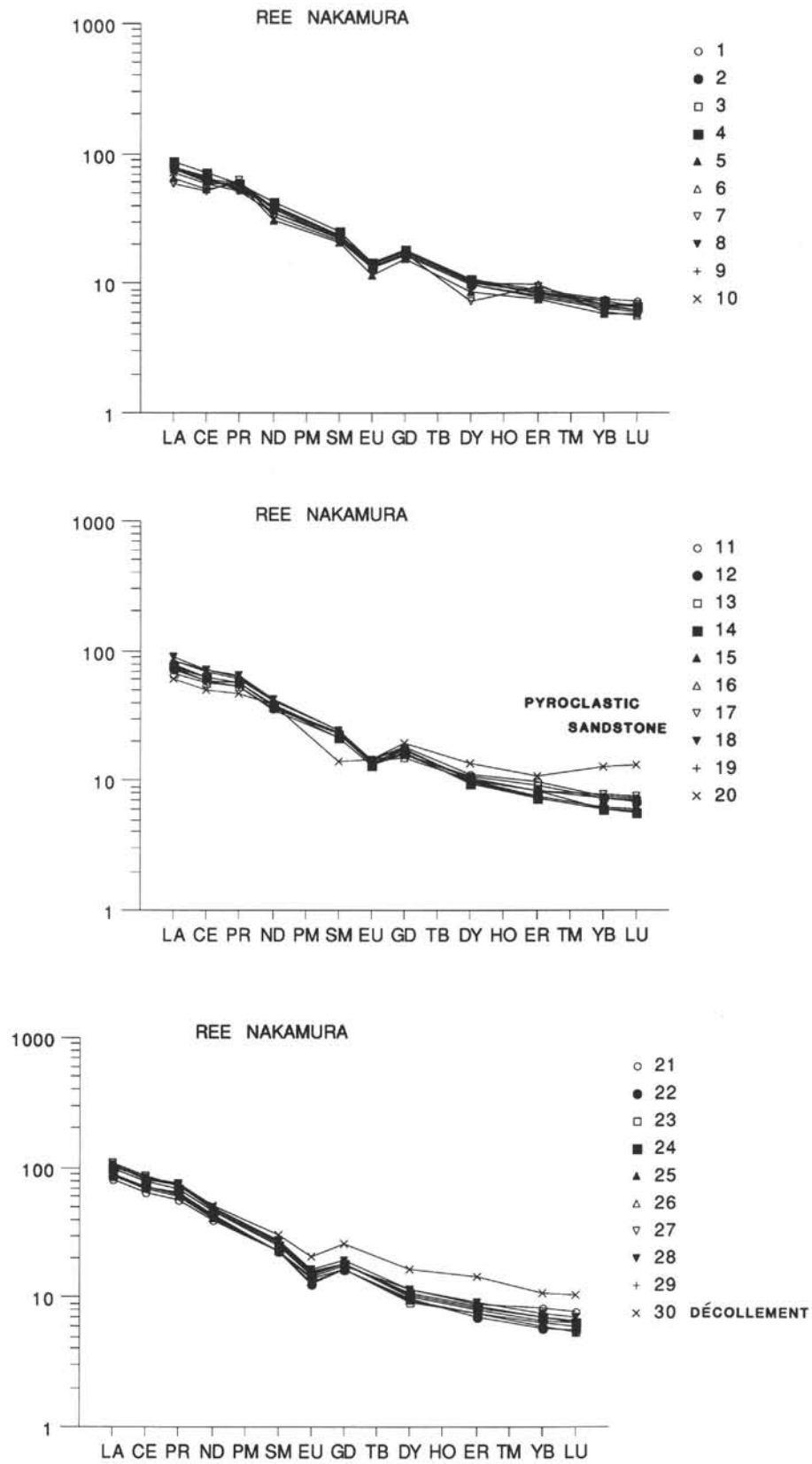


Figure 2. Chondrite normalized (Nakamura, 1974) REE abundances for 49 sediment samples, mainly mud, throughout Site 808, grouped for clarity in tens. Note that the few primary volcanic sands and ashes analyzed show typical higher total abundances of REE, with pyroclastic sand showing large negative Eu anomaly. Also note that three out of four mud samples from the ~20-m-thick décollement show enhanced heavy REE abundances.

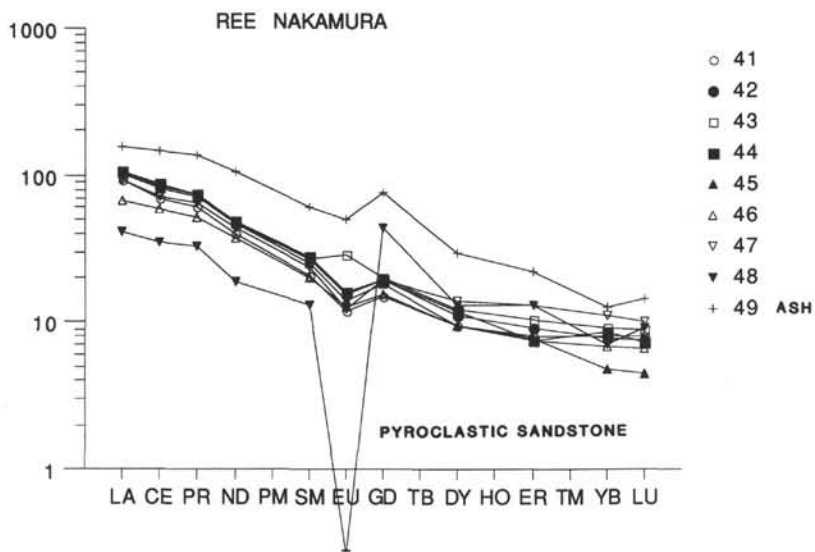
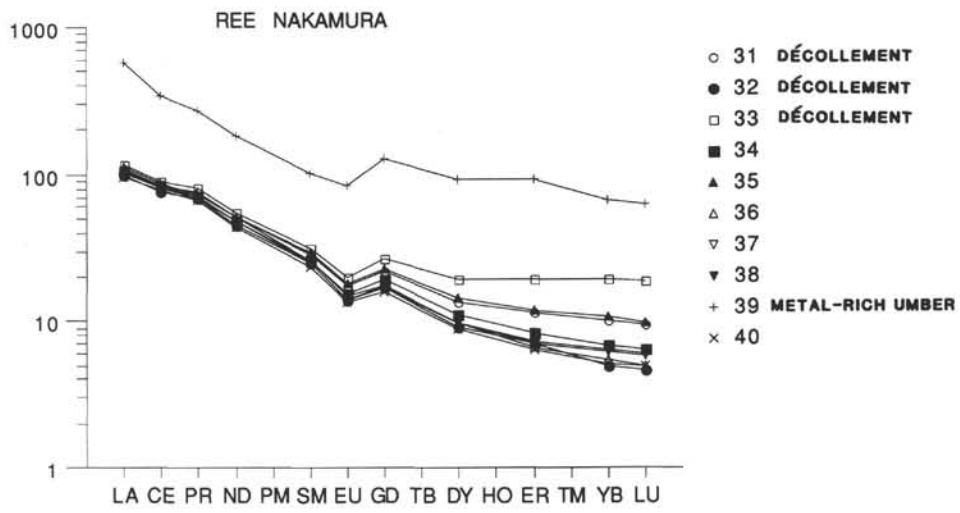


Figure 2 (continued).

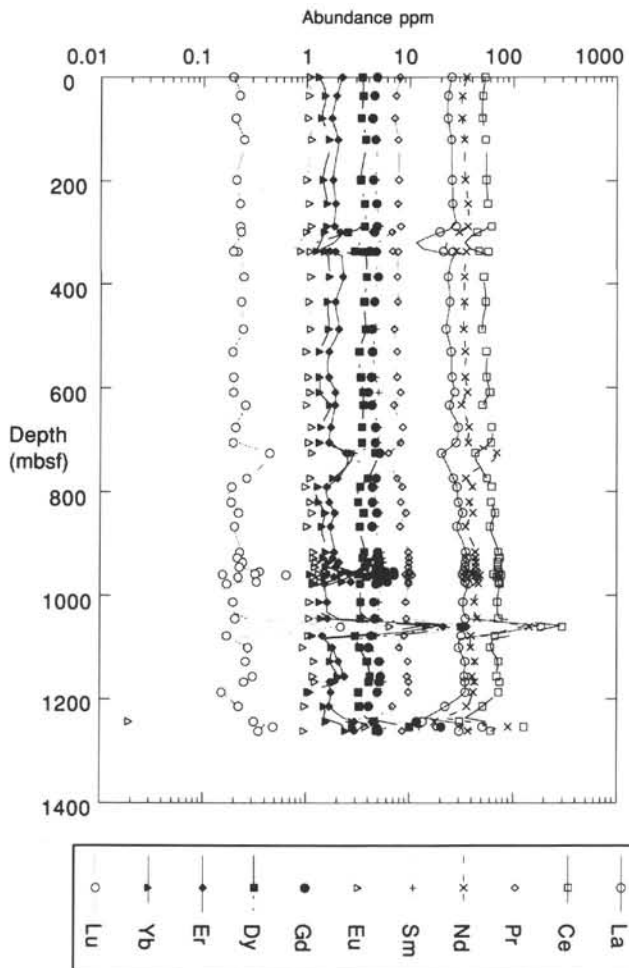


Figure 3. Rare-earth-element abundances (ppm) vs. depth (mbsf) for Site 808. Logarithmic axes used to clarify abundance data. Note the dramatic increase in abundances in the interval at ~1060 mbsf, associated with a metalliferous brown mud, also enriched in Ca, Fe, Mg, Mn, and P oxides.